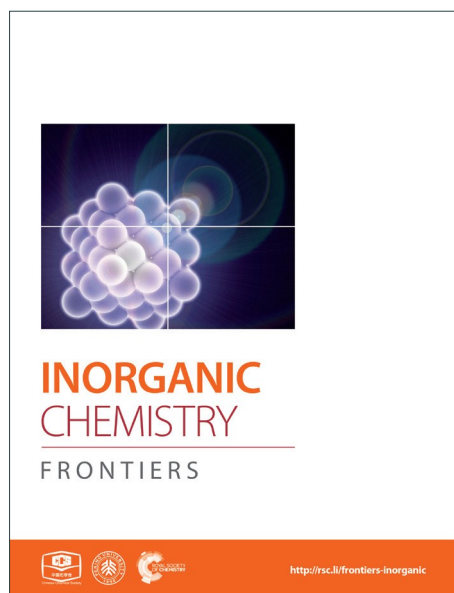
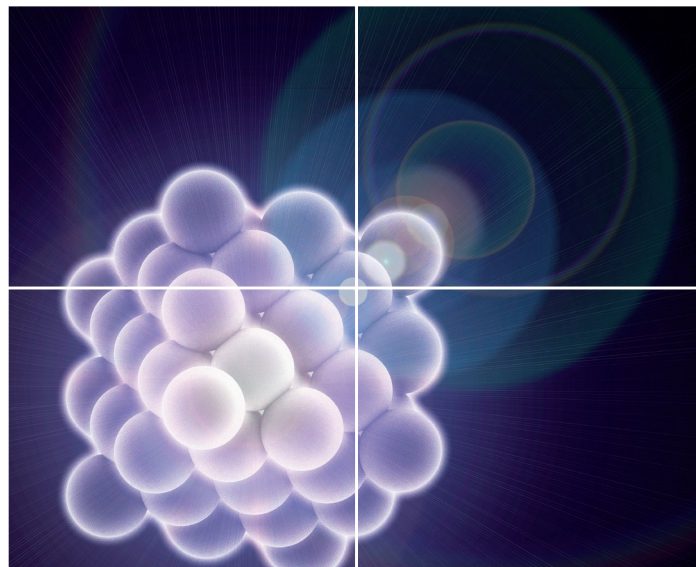


INORGANIC CHEMISTRY

FRONTIERS

Accepted Manuscript



This is an *Accepted Manuscript*, which has been through the Royal Society of Chemistry peer review process and has been accepted for publication.

Accepted Manuscripts are published online shortly after acceptance, before technical editing, formatting and proof reading. Using this free service, authors can make their results available to the community, in citable form, before we publish the edited article. We will replace this *Accepted Manuscript* with the edited and formatted *Advance Article* as soon as it is available.

You can find more information about *Accepted Manuscripts* in the [Information for Authors](#).

Please note that technical editing may introduce minor changes to the text and/or graphics, which may alter content. The journal's standard [Terms & Conditions](#) and the [Ethical guidelines](#) still apply. In no event shall the Royal Society of Chemistry be held responsible for any errors or omissions in this *Accepted Manuscript* or any consequences arising from the use of any information it contains.



Journal Name

ARTICLE

Single-molecule magnet involving strong exchange coupling in terbium(III) complex with 2,2'-bipyridin-6-yl *tert*-butyl nitroxide

Takuya Kanetomo,^a Shunsuke Yoshii,^b Hiroyuki Nojiri^b and Takayuki Ishida^{a,*}Received 00th January 20xx,
Accepted 00th January 20xx

DOI: 10.1039/x0xx00000x

www.rsc.org/

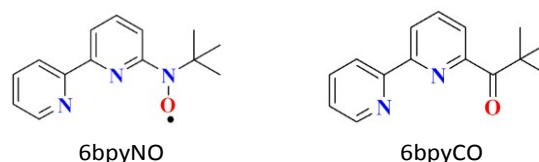
A novel terbium(III)-radical complex [Tb^{III}(hfac)₃(6bpyNO)] (**Tb-6bpyNO**; 6bpyNO = 2,2'-bipyridin-6-yl *tert*-butyl nitroxide) was synthesized. The intramolecular antiferromagnetic interaction in **Tb-6bpyNO** was confirmed by comparison with the magnetic properties of [Tb^{III}(hfac)₃(6bpyCO)] (**Tb-6bpyCO**; 6bpyCO = 2,2'-bipyridin-6-yl *tert*-butyl ketone) together with [Y^{III}(hfac)₃(6bpyNO)]. **Tb-6bpyNO** showed a hysteresis loop with negligible coersivity below 1.6 K. The dispersion of magnetic susceptibility with an applied bias field of 2000 Oe gave the energy barrier $E_a/k_B = 21.1(8)$ K. In contrast, **Tb-6bpyCO** did not behave as a single-molecule magnet, despite practically the same crystal field.

Introduction

Molecule-based magnetic materials have an advantage in arranging a variety of magnetic orbitals, which results in single-molecule magnets (SMMs) as well as interesting exchange-coupled systems.¹ Recently, 4f-ion-based heterospin compounds have been intensively studied for development of SMMs^{2,3}, because strong magnetic anisotropy and large magnetic moment are available from lanthanoid (Ln) ions.⁴ When the spin centre of a paramagnetic ligand is bonded to a metal ion, the metal-radical complex shows strong exchange coupling via direct coordination. The 6bpyNO radical (6bpyNO = 2,2'-bipyridin-6-yl *tert*-butyl nitroxide; Scheme 1) has been synthesized for obtaining the strong exchange coupling in transition metal-radical complexes.⁵ Recently, lanthanoid-radical complexes (4f-2p heterospin systems) have been the subjected of intense research activity.^{6,7} We utilize 6bpyNO as a component of 4f-2p systems and found that [Gd^{III}(hfac)₃(6bpyNO)] (abbreviated as **Gd-6bpyNO** hereafter; Hhfac = 1,1,1,5,5,5-hexafluoropentane-2,4-dione) possesses the largest exchange coupling ($2J/k_B = -15.9(2)$ K) in the Gd-nitroxide coordination compounds ever reported.⁸

In the present work, we have synthesized the corresponding Tb analogue, **Tb-6bpyNO**, and investigated the magnetic properties to understand the role of the ligand spin introduced to SMMs, which would be useful to create new heterospin compounds and SMMs. The present work also covers the empirical $\Delta(\chi_m T)$ method⁹ using 2p-spin masked 6bpyCO (2,2'-bipyridin-6-yl *tert*-butyl ketone; Scheme 1) and clarifies the nature of intramolecular Tb-radical exchange coupling.

Scheme 1. Structural formula of 6bpyNO and 6bpyCO.



Results and discussion

Synthesis and description of the crystal structure

We synthesized **RE-6bpyNO** (RE = Tb, Y) according to the method developed for the RE = Gd analogue with a slight modification.⁸ Y³⁺ ion has often been used for a diamagnetic metal centre because the ionic radius is close to those of heavy lanthanide ions (0.90 Å for Y³⁺ vs 0.94 Å for Gd³⁺ and 0.92 Å for Tb³⁺).¹⁰ The products are stable at room temperature under air. Their fine crystals were obtained and subjected without further purification to spectroscopic, X-ray crystallographic and magnetic analyses. The crystallography results are given in Table 1. **RE-6bpyNO** (RE = Tb, Y) crystallizes in a monoclinic $P2_1/n$ space group, being completely isomorphous to **Gd-6bpyNO** (Fig. 1a).

The RE³⁺ centre is nine-coordinated including two RE-N and one RE-O bonds from the chelate ligand 6bpyNO. Other six bonds involve oxygen atoms from three hfac coligands. The coordination polyhedron can be best described as a capped square antiprism (CSAPR) with N2 as a cap (Fig. 1c). We further confirmed the CSAPR structure around the Tb and Y ions \ddagger on the SHAPE program.¹¹ A magnetic axial anisotropy is expected in the CSAPR structure. Important geometrical parameters possibly relating to the intermolecular 4f-2p exchange coupling, such as bond lengths (RE-O1, RE-N1 and RE-N2), bond angles (RE1-O1-N1) and torsion angles (RE1-O1-N1-C1), are summarized in Table 1.

^aDepartment of Engineering Science, The University of Electro-Communications, Tokyo 182-8585, Japan.

^bInstitute of Materials Research, Tohoku University, Katahira, Sendai 980-8577, Japan.

* Corresponding author. Tel.: +81 42 443 5490; fax.: +81 42 443 5501. E-mail address: takayuki.ishida@uec.ac.jp

Table 1. Selected crystallographic data, bond lengths (Å), bond angles (°) and torsion angles (°) for **RE-6bpyNO** (RE = Gd³⁺, Tb, Y) and **Tb-6bpyCO**.

Compound	Gd-6bpyNO ^{a)}	Tb-6bpyNO	Y-6bpyNO	Tb-6bpyCO	
Formula	C ₂₉ H ₁₉ F ₁₈ N ₃ O ₇ Gd	C ₂₉ H ₁₉ F ₁₈ N ₃ O ₇ Tb	C ₂₉ H ₁₉ F ₁₈ N ₃ O ₇ Dy	C ₂₉ H ₁₉ F ₁₈ N ₃ O ₇ Dy	
Formula weight	1020.71	1022.38	952.36	1020.39	
T / K	100	100	100	100	
Crystal system	Monoclinic	Monoclinic	Monoclinic	Monoclinic	
Space group	<i>P</i> 2 ₁ / <i>n</i>				
<i>a</i> / Å	13.467(3)	13.433(2)	13.392(2)	13.456(3)	
<i>b</i> / Å	17.045(4)	17.068(3)	17.074(3)	17.130(3)	
<i>c</i> / Å	16.692(4)	16.695(2)	16.648(2)	16.654(3)	
β / deg	105.43(1)	105.208(7)	105.114(7)	105.460(8)	
<i>V</i> / Å ³	3694(2)	3693.8(9)	3675.0(9)	3700(1)	
<i>Z</i>	4	4	4	4	
<i>D</i> _{calc} / g cm ⁻³	1.835	1.838	1.721	1.832	
μ (MoK α) / mm ⁻¹	1.939	2.049	1.728	2.045	
<i>R</i> (<i>F</i>) ^{b)} (<i>I</i> > 2 σ (<i>I</i>))	0.0463	0.0424	0.0633	0.0340	
<i>R</i> _w (<i>F</i> ²) ^{c)} (all data)	0.0482	0.0530	0.0855	0.0434	
Goodness-of-fit	1.148	1.098	1.037	1.077	
RE1-O1 / Å	2.373(4)	2.365(4)	2.333(3)	Tb1-O1 / Å	2.396(3)
RE1-N2 / Å	2.560(4)	2.550(3)	2.539(3)	Tb1-N1 / Å	2.569(3)
RE1-N3 / Å	2.568(4)	2.547(4)	2.539(4)	Tb1-N2 / Å	2.559(3)
RE1-O1-N1 / deg	126.2(3)	126.3(3)	126.1(3)	Tb1-O1-C30 / deg	127.8(2)
RE1-O1-N1-C1 / deg	-16.5(5)	-16.6(5)	-15.4(5)	Tb1-O1-C30-C1 / deg	-13.1(4)

^{a)} Ref. 8. ^{b)} $R = \sum ||F_o| - |F_c|| / \sum |F_o|$. ^{c)} $R_w = [\sum w(F_o^2 - F_c^2)^2 / \sum w(F_o^2)^2]^{1/2}$.

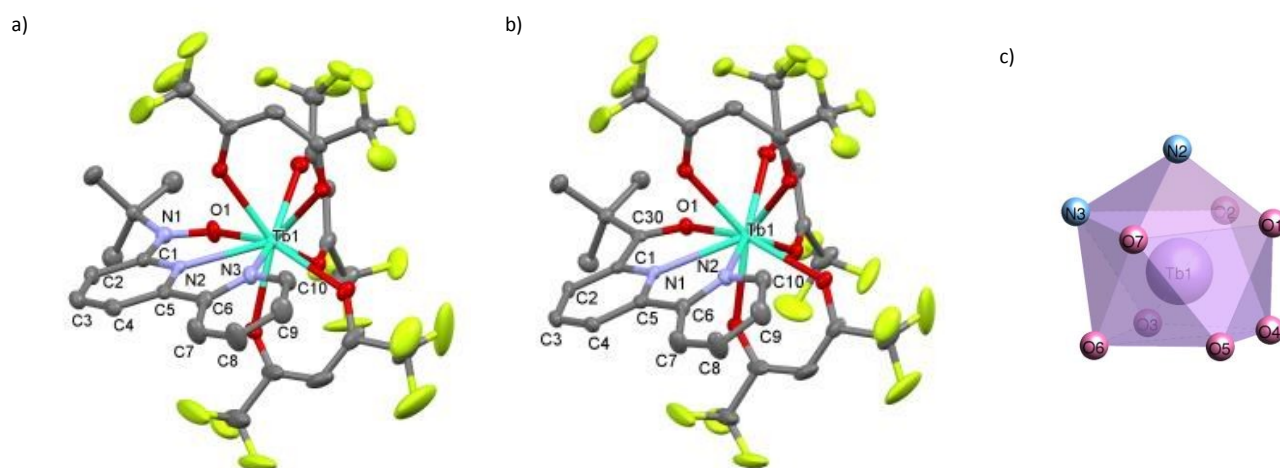


Fig. 1. X-ray structures of (a) **Tb-6bpyNO** and (b) **Tb-6bpyCO**. Thermal ellipsoids are drawn at the 50% probability level. Hydrogen atoms are omitted for the sake of clarity. (c) Capped square antiprism structure in **Tb-6bpyNO**.

We also prepared and characterized **Tb-6bpyCO** (Fig. 1b) as a radical-spin silent reference. The crystallographic analysis clarified that it was isostructural to the 6bpyNO analogues (Table 1). A carbonyl group (C30-O1 in Fig. 1b) provides a ligating oxygen atom in place of the nitroxide group (N1-O1 in Fig. 1a). The Tb ion in **Tb-6bpyCO** also has a CSAPR structure. Furthermore the shape measures for **Tb-6bpyNO** and **Tb-6bpyCO** are quite close to each other, in particular 0.241 and 0.249, respectively, for CSAPR, according to the SHAPE program.¹¹ This finding suggests that **Tb-6bpyCO** is a suitable model reproducing the crystal field around the Tb ion in **Tb-6bpyNO**.

Magnetic properties

The direct current (dc) magnetic susceptibilities of **Tb-6bpyNO**, measured at an applied magnetic field of 5000 Oe in a temperature range 1.8 - 300 K, are displayed in Fig. 2. The specimen was fixed with a small amount of mineral oil. At 300 K, the $\chi_m T$ value was 11.5 cm³ K mol⁻¹ for **Tb-6bpyNO**. This is close to the theoretical values at the high-temperature limit (12.2 cm³ K mol⁻¹ as the sum from $J^2 = 6$, $g_J = 3/2$ for a free Tb³⁺ ion and $S = 1/2$, $g = 2$ for an organic radical). On cooling, the $\chi_m T$ values monotonically decreased to 5.17 cm³ K mol⁻¹ at 2 K. Since we used powder samples, the major part of the reduction is caused by the anisotropy of Ln ions. It should be noted that the $\chi_m T$ value of a radical spin is as small as 0.38 cm³ K mol⁻¹ and minor to the large reduction.

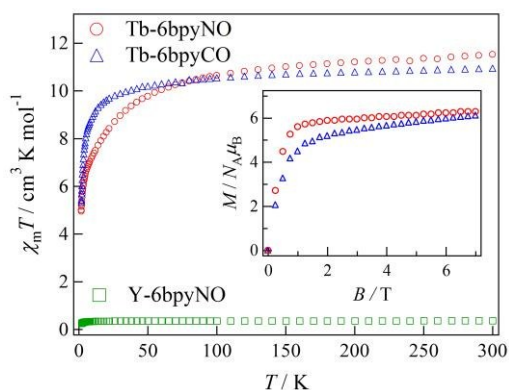


Fig. 2. Temperature dependence of $\chi_m T$ for **Tb-6bpyNO** (red circle), **Y-6bpyNO** (green square) and **Tb-6bpyCO** (blue triangle), measured at 5000 Oe.

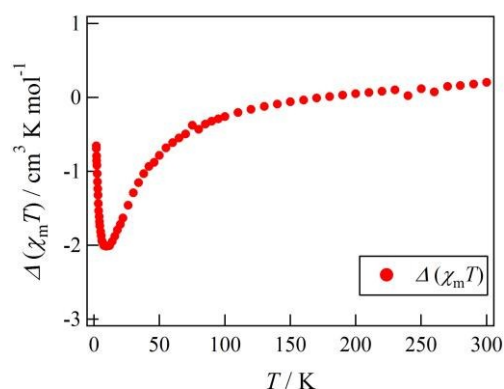


Fig. 3. Temperature dependence of $\Delta(\chi_m T)$ as defined by $\Delta(\chi_m T) = (\chi_m T)_{\text{Tb-6bpyNO}} - (\chi_m T)_{\text{Y-6bpyNO}} - (\chi_m T)_{\text{Tb-6bpyCO}}$.

We tried to obtain a clue to the nature of the magnetic coupling by a conventional approach. In the 4f-3d heterospin systems there has been an empirical method known, where the $\chi_m T$ difference between the heterospin compound and 3d-spin masked reference is evaluated.⁹ On the other hand, the corresponding research for 4f-2p systems is somewhat rare.¹² Some “nitronyl nitroxide” complexes have been modelled with nitronyl complexes^{12,13} (“nitronyl nitroxide” stands for 4,4,5,5-tetramethylimidazolin-1-oxyl 3-oxide). Alternatively, a succinimide has also been proposed as a diamagnetic model.¹⁴ In the present case, 6bpyCO is rationally assumed as a diamagnetic reference for 6bpyNO.

Actually, **Tb-6bpyCO** was found to be isomorphous to **Tb-6bpyNO** (see above). The results of magnetic susceptibility of two model compounds are superposed in Fig. 2. The data on **Tb-6bpyCO** involve only the contribution of Tb^{3+} with the single-ion magnetic anisotropy regulated by the crystal field, and the data on **Y-6bpyNO** contain only the contribution of radical spin affected by the radical-radical intermolecular interaction. Hence, the difference $\Delta(\chi_m T) = (\chi_m T)_{\text{Tb-6bpyNO}} - (\chi_m T)_{\text{Y-6bpyNO}} - (\chi_m T)_{\text{Tb-6bpyCO}}$ implies the nature of the overall exchange interactions between Tb^{3+} and radical spins. Positive and negative values of the $\Delta(\chi_m T)$ are directly related to ferro- and antiferromagnetic interactions, respectively. The temperature dependence of $\Delta(\chi_m T)$ is displayed in Fig. 3. The $\Delta(\chi_m T)$ value shows large negative value in the wide range

below ca. 250 K. At the lowest temperature region below 10 K, an upturn appeared, possibly being ascribed to the effect of intermolecular interactions or slight difference of crystal fields between **Tb-6bpyNO** and **Tb-6bpyCO**.

The field dependence of magnetizations measured by SQUID at 1.8 K is shown in the inset of Fig. 2. The specimens were not fixed, so that the microcrystalline specimens would be aligned in the field direction. The magnetizations tend to saturate in higher fields and the value was $6.28 \mu_B$ at 7 T for **Tb-6bpyNO**. The expected value gives $8 \mu_B$ as the subtraction of those between a free Tb^{3+} ion and 6bpyNO radical. There are two molecular directions in a unit cell, and the CSAPR principal axes are canted by 43° to each other, which is estimated by the Tb1-N2 bond directions. Thus, we have to reduce the saturation moments about 7% from those of the single site values, giving $7.4 \mu_B$. The reduction of the measured magnetization may be caused by the imperfect field-alignment. The magnetization of **Tb-6bpyCO** also shows gradual saturation and the value was $6.12 \mu_B$ at 7 T. The larger slope found around 7 T is compatible with the uncompensated magnetization of Tb^{3+} ions. However, it is difficult to distinguish between the effect of intramolecular exchange coupling and that of the Tb^{3+} single ion anisotropy from these magnetization curves.

Let us compare the strong antiferromagnetic coupling found in the present system with the result of a similar system. Another 4f-2p heterospin system, $[\text{RE}^{\text{III}}(\text{hfac})_3(2\text{pyNO})]$ (**RE-2pyNO**), has been developed by use of *tert*-butyl 2-pyridyl nitroxide (2pyNO).^{15,16} Relatively strong antiferromagnetic 4f-2p exchange coupling was characterized in **Gd-2pyNO**¹⁵ like **Gd-6bpyNO**.⁸ Antiferromagnetic coupling in **Tb-2pyNO** was precisely evaluated by means of inelastic neutron scattering and high-frequency electron paramagnetic resonance.¹⁷ In the 6bpyNO system, although conventional experimental methods were utilized, **Gd-** and **Tb-6bpyNO** were both clarified to have intramolecular antiferromagnetic coupling. It is likely that the antiferromagnetic coupling is considerable in **Tb-6bpyNO** from the notably negative $\Delta(\chi_m T)$ even around 100 K. This notion is consistent with the empirical rule that the sign of exchange coupling is common among the heterospin molecules of Gd^{3+} and heavy lanthanide ions coupled with 3d transition metal ions¹⁸ and radicals.¹⁷ Unfortunately, the $\Delta(\chi_m T)$ method could not afford quantitative information any further.

Dynamic magnetic properties

The pulsed-field magnetization experiments¹⁹ on **Tb-6bpyNO** were carried out by using a ^3He cryostat (Fig. 4). Hysteresis and magnetization jumps were found at 0.5 and 1.6 K, and the derivative of the magnetization clarifies the apparent coercive field of about 0.5 T. The field position depends slightly on temperature and field-sweeping rate, which shows the role of the thermal relaxation.

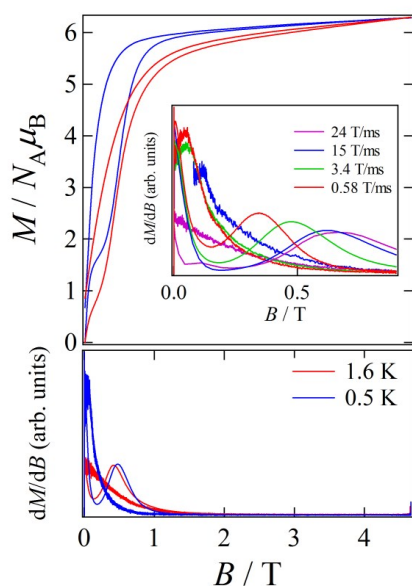


Fig. 4. Pulsed-field magnetizations curve (top) and the corresponding dM/dB vs B plot (bottom) for **Tb-6bpyNO** measured at 0.5 and 1.6 K. The inset shows the corresponding dM/dB vs B plot for **Tb-6bpyNO** at various field-sweeping rates.

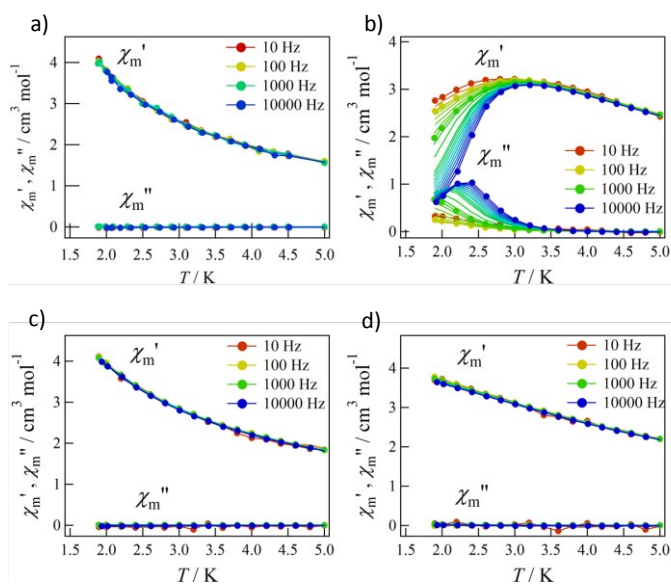


Fig. 5. AC magnetic susceptibilities for **Tb-6bpyNO** at applied dc bias fields of (a) 0 Oe and (b) 2000 Oe and for **Tb-6bpyCO** at applied dc bias fields of (c) 0 Oe and (d) 2000 Oe.

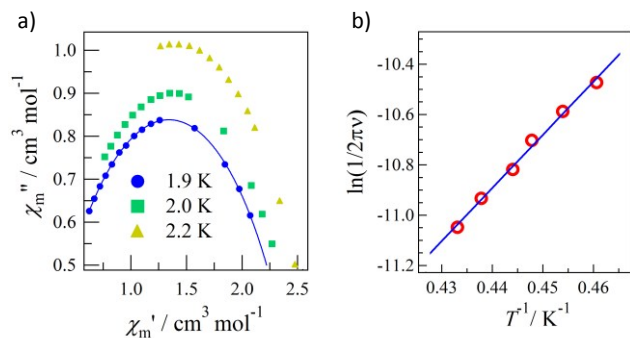


Fig. 6. (a) Cole-Cole plot and (b) Arrhenius plot for **Tb-6bpyNO**.

As the applied field was removed, the magnetization quickly disappeared (Fig. 4); namely, the coercivity does not appear as bulk. It should be noted that the down sweep is much slower than the up sweep for the non-symmetric pulse shape. To investigate the dynamics on the magnetization reversal, we measured the alternating current (ac) magnetic susceptibility. Figure 5a shows the in-phase and out-of-phase portions of the ac magnetic susceptibility (χ_m' and χ_m'' , respectively) for **Tb-6bpyNO**, measured without any applied dc field. No appreciable χ_m'' was recorded, being consistent with the fast relaxation of magnetization found in the pulsed-field experiments. On the other hand, when a direct current (dc) bias field²⁰ of 2000 Oe was applied, a decrease of χ_m' and concomitant increase of χ_m'' were recorded (Fig. 5b). Frequency dependence was also observed. When we plotted the χ_m'' against χ_m' at various temperatures according to the Cole-Cole analysis,²¹ a semicircle was drawn at 1.9 K with $\alpha = 0.236(2)$ (Fig. 6a). The α value in the Debye model is relatively small in $\chi(\omega) = \chi_s + (\chi_T - \chi_s) / (1 + (1/\omega\tau)^{1-\alpha})$, where χ_T and χ_s are the isothermal and adiabatic susceptibilities, respectively.²² This finding guarantees a single relaxation process in each molecule. The Arrhenius plot for **Tb-6bpyNO** shows a straight line from the data of the χ'' peak (Fig. 6b), and the activation energy (E_a) for the magnetization reversal was estimated as $E_a/k_B = 21.1(8)$ K with $\tau_0 = 1.7(6) \times 10^{-9}$ s, where τ_0 stands for the pre-exponential factor in the Arrhenius equation, $\ln(2\pi\nu) = \ln(\tau_0) + E_a/k_B$.²³

In the magnetic field, the splitting of the lowest doublet causes the Zeeman energy gap. For $7.4 \mu_B/\text{molecule}$ and 2000 Oe the gap is about 2 K. This gap is minor to the gap obtained by the Arrhenius plot, and the main source of the activation energy is the anisotropy of the **Tb-6bpyNO** molecule as a SMM.

A square antiprismatic (SAPR) coordination polyhedron seems to be suitable for the strong axial anisotropy and the energy gap is quite large between the ground state ($J^2 = 6$) and lowest-excited state ($J^2 = 5$) for a Tb^{3+} ion.^{4,24,25} It has already been clarified that SAPR-configured **Tb-2pyNO** was a SMM.¹⁶ In the present work, the coordination structure of **Tb-6bpyNO** belongs to CSAPR, which is similar to SAPR. It is natural that both **Tb-6bpyNO** and **Tb-2pyNO** behave as SMMs. However, the crystal field effect is not a decisive factor, as follows.

Tb-6bpyNO affords one of the best venues where we assess the role of paramagnetic ligand in SMMs by comparing the reference compound with the 2p-spin masked. The ac magnetic susceptibility measurements on **Tb-6bpyCO** displayed no χ_m'' at 0 Oe or even at 2000 Oe dc bias field (Figs. 5c and 5d). This remarkable difference is hard to understand because the energy barrier caused by the Tb^{3+} anisotropy should be nearly identical between **Tb-6bpyNO** and **Tb-6bpyCO**. Long *et al.* have noted that the bistability is not guaranteed for a non-Kramers Tb^{3+} ion and accordingly the crystal field is required so that Tb^{3+} could acquire axial magnetic anisotropy.²⁴ If the strong axial magnetic anisotropy presents, both **Tb-6bpyNO** and **Tb-6bpyCO** should behave as SMMs, which contradicts to the present experimental results. At this point it is noticed that the even/odd of the total magnetic moment is different between two species, which is

related to the Kramers theorem. The ground total spin of **Tb-6bpyNO** is 5/2 (a Kramers molecule) whilst that of **Tb-6bpyCO** is 3 (a non-Kramers molecule), assuming that the spin-spin coupling is strong enough, compared with cryogenic temperatures.

The presence of a 2p spin is critical for the SMM performance in the present study. One may remind the studies on $[\text{Tb}(\text{pc})_2]^0$ and $[\text{Tb}(\text{pc})_2]^-$ (pc = phthalocyaninate).^{4,26} Only the former has a delocalized π spin on the (pc)₂ moiety. The SMM performance of the former was found to be better,²⁶ which can be also interpreted by a odd/even nature of the ground state moments. Another example is found in the fact that SMM behaviour on **Dy-2pyNO** or **Dy-6bpyNO** has never been reported.¹⁶ In fact, no meaningful χ_m'' was observed for **Dy-2pyNO** or **Dy-6bpyNO** (Figures S1 and S2, Electronic Supplementary Information). The establishment of the parity effect may need further theoretical clarification, but the control of the relaxation by radical spin modification would lead to new functionality of molecule-based magnets.

Finally we comment on the comparison with **Tb-2pyNO** showing large coercivity and slow magnetization reversal in ac magnetic susceptibility.¹⁶ It is known that the magnetization reversal is sensitive to the relaxations caused by the hyperfine couplings,²⁷ dipolar interactions in Ln ions,²⁸ and weak f-d and f-p exchange couplings.^{29,30} It is noticed that the CSAPR principal axes of monoclinic **Tb-6bpyNO** are canted by 43° between neighbouring molecules. On the other hand, **Tb-2pyNO** crystallizing in a triclinic *P*-1 space group¹⁶ exhibits a cant angle of ca. 5° between two independent molecules. This difference may affect on the relaxation with the dipolar interactions and the intramolecular interaction. It is because the transverse components of fluctuating magnetic fields dominating the relaxation are enhanced by the tilting of the principle axes.

Conclusions

We have successfully prepared **Tb-6bpyNO** as an exchange-involving SMM or single-ion magnet. The intramolecular antiferromagnetic coupling was indicated by the empirical $\Delta(\chi_m T)$ method after the corresponding carbonyl compound was proposed as a 2p-spin-masked reference. **Tb-6bpyNO** behaved as a SMM with $E_a/k_B = 21.1(8)$ K and $\tau_0 = 1.7(6) \times 10^{-9}$ s at the external dc bias of 2000 Oe. The 4f-2p heterospin approach seems to be one of promising strategies toward novel SMMs. The relaxation by the parity effect is also discussed in terms of the marked difference of SMM characteristics with and without a radical spin.

Experimental section

Synthesis

6bpyNO was synthesized by the method reported in the literature.⁵ Complexes **RE-6bpyNO** (RE = Tb, Y) were prepared from $[\text{RE}^{\text{III}}(\text{hfac})_3(\text{H}_2\text{O})_2]$ (RE = Tb, Y)³¹ and 6bpyNO in a

dichloromethane - *n*-heptane mixed solvent, according to the procedure known for the Gd analogue.⁸

[Tb^{III}(hfac)₃(6bpyNO)] (Tb-6bpyNO). The yield was 58%. Mp. 140–146 °C (decomp.). Anal. Calcd. for C₂₉H₁₉N₃O₇F₁₈Tb: C, 34.07; H, 1.87; N, 4.11%. Found: C, 33.74; H, 1.70; N, 3.99%. IR (neat, attenuated total reflection (ATR)) 1651, 1488, 1249, 1190, 1133, 1096, 795, 773, 659, 582 cm⁻¹.

[Y^{III}(hfac)₃(6bpyNO)] (Y-6bpyNO). The yield was 61%. Mp. 168–170 (decomp.) °C. Anal. Calcd. for C₂₉H₁₉N₃O₇F₁₈Y: C, 36.57; H, 2.01; N, 4.41%. Found: C, 36.07; H, 2.22; N, 4.35%. IR (neat, ATR) 1655, 1491, 1251, 1190, 1137, 1099, 796, 773, 660, 584 cm⁻¹.

2,2'-bipyridin-6-yl tert-butyl ketone (6bpyCO). 6bpyCO was prepared according to the synthesis of *tert*-butyl 2-(5-methylpyridyl) ketone,³² using 6-bromo-2,2'-bipyridine in place of 2-bromo-5-methylpyridine as a starting material. To a suspension of 6-bromo-2,2'-bipyridine (2.52 g, 10.7 mmol) in dry ether (30 mL) was added dropwise *n*-BuLi (1.60 mol L⁻¹ in *n*-hexane, 7.4 mL, 12 mmol) at -76 °C. The mixture was stirred at -76 °C for 1 h, and the resultant solution was added dropwise to a solution of pivaloyl chloride (2.6 mL, 21 mmol) in dry THF (5 mL). The mixture was stirred at 0 °C for 15 h and then further stirred at room temperature for 2 h. The reaction mixture was quenched with cooled water followed by cold 40% NaOH aqueous solution, and stirred for 30 min. After the aqueous layer was extracted with ether, the combined organic layer was dried over anhydrous MgSO₄. The filtrate is concentrated under reduced pressure, and the resulting brown oil was purified through HPLC (1H + 2H (Japan Analytical Industry, eluted with CHCl₃) to yield green oil. The yield was 422 mg (1.76 mmol, 16%). ¹H NMR (500 MHz, CDCl₃): δ 8.69 (dd, *J* = 4.2, 1.6 Hz, 1 H), 8.56 (dd, *J* = 7.7, 1.7 Hz, 1 H), 8.42 (d, *J* = 7.9 Hz, 1 H), 7.95 (dd, *J* = 7.7, 1.7 Hz, 1 H), 7.93 (t, *J* = 7.7 Hz, 1 H), 7.86 (td, *J* = 7.7, 1.6 Hz, 1 H), 7.33 (ddd, *J* = 7.7, 4.2, 1.6 Hz, 1 H), 1.55 (s, 9 H). ¹³C NMR (126 MHz, CDCl₃): δ 206.4, 155.6, 154.2, 153.7, 149.2, 137.8, 137.0, 124.0, 123.7, 123.2, 121.0, 44.2, 27.7. IR (neat, ATR): 2956, 1685, 1578, 1479, 1428, 1201, 993, 970, 792, 757 cm⁻¹.

[Tb^{III}(hfac)₃(6bpyCO)] (Tb-6bpyCO). **Tb-6bpyCO** was prepared according to the procedure of **RE-6bpyNO** using $[\text{Tb}^{\text{III}}(\text{hfac})_3(\text{H}_2\text{O})_2]$ and 6bpyCO as starting materials. The yield was 14%. Mp. 191–193 °C (decomp.). Anal. Calcd. for C₃₀H₁₉N₂O₇F₁₈Tb: C, 35.31; H, 1.88; N, 2.75%. Found: C, 35.19; H, 1.91; N, 2.62%. IR (neat, ATR) 1651, 1489, 1249, 1189, 1133, 1096, 795, 765, 659, 582 cm⁻¹.

X-ray crystallography

X-ray diffraction data of **RE-6bpyNO** (RE = Tb, Y) and **Tb-6bpyCO** were collected on a Rigaku Saturn70 CCD diffractometer with graphite monochromated MoK α radiation ($\lambda = 0.71073$ Å). The structures were directly solved by a heavy-atom method and expanded using Fourier techniques in the CrystalStructure program package.³³ Numerical absorption correction was used. All of the hydrogen atoms were located at calculated positions and the parameters were refined as "riding." The thermal displacement parameters of non-hydrogen atoms were refined anisotropically. Selected

crystallographic data and geometrical parameters are listed in Table 1. CCDC numbers 1011564, 1404995 and 1404996.

Magnetic measurements

The dc magnetic susceptibilities and magnetizations of polycrystalline specimens of **RE-6bpyNO** (RE = Tb, Y) and **Tb-6bpyCO** were measured on a Quantum Design MPMS-XL SQUID magnetometer equipped with a 7 T coil in a temperature range 1.8 - 300 K. The magnetic data were corrected with diamagnetic blank data of the sample holder measured separately. The diamagnetic contribution of the sample itself was estimated from Pascal's constants. Ac magnetic susceptibilities were recorded on a Quantum Design PPMS ac magnetometer.

Low-temperature magnetization was measured by a conventional inductive probe in pulsed-magnetic fields, and the temperature was reached as low as 0.5 K using a ³He cryostat.¹⁹ Polycrystalline specimens were mounted in a capillary made of polyimide. The samples were not fixed within the sample tube and then they aligned in the magnetic field direction. After we applied the magnetic field several times, the orientation effect was saturated, and the magnetization curves obtained in further shots were found to be identical. The magnetization was calibrated by independent measurements on a SQUID magnetometer.

Acknowledgement

T. K. was supported by the JSPS program for Research Fellowships for Young Scientist (No. 15J11497).

Notes and references

† CCDC numbers 1011564, 1404995 and 1404996 contain the supplementary crystallographic data for complexes **Tb-**, **Y-6bpyNO** and **Tb-6bpyCO**, respectively. These data can be obtained free of charge via <http://www.ccdc.cam.ac.uk/conts/retrieving.html>, or from the Cambridge Crystallographic Data Centre, 12 Union Road, Cambridge CB2 1EZ, UK; fax: (+44) 1223-336-033; or e-mail: deposit@ccdc.cam.ac.uk.

‡ Shape measures were 0.241 (CSAPR) and 1.053 (TCTPR); tricapped trigonal prism for **Tb-6bpyNO**, 0.235 (CSAPR) and 1.023 (TCTPR) for **Y-6bpyNO**, and 0.249 (CSAPR) and 1.019 (TCTPR) for **Tb-6bpyCO**.

- O. Kahn, *Molecular Magnetism*, VCH Publications, New York, 1993; J. S. Miller and M. Eds, *Magnetism Molecules to Materials I – V*, Wiley-VCH, Weinheim, Germany, 1999-2005.
- D. Gatteschi, R. Sessoli and J. Villan, *Molecular Nanomagnets*, Oxford University Press, New York, 2006; D. Gatteschi and R. Sessoli, *Angew. Chem. Int. Ed.*, 2003, **42**, 2003.
- S. Osa, T. Kido, N. Matsumoto, N. Re, A. Pochaba and J. Mrozinski, *J. Am. Chem. Soc.*, 2004, **126**, 420; F. Pointillart, K. Bernot, R. Sessoli and D. Gatteschi, *Chem. –Eur. J.*, 2007, **13**, 1602.
- F. Mori, T. Ishida and T. Nogami, *Polyhedron*, 2005, **24**, 2588; F. Mori, T. Nyui, T. Ishida, T. Nogami, K. –Y. Choi and H. Nojiri, *J. Am. Chem. Soc.*, 2006, **128**, 1440; S. Ueki, T. Ishida, T. Nogami, K. –Y. Choi and H. Nojiri, *Chem. Phys. Lett.*, 2007, **440**, 263.
- N. Ishikawa, M. Sugita, T. Ishikawa, S.–y. Koshihara and Y. Kaizu, *J. Am. Chem. Soc.*, 2003, **125**, 8694.
- K. Osanai, A. Okazawa, T. Nogami and T. Ishida, *J. Am. Chem. Soc.*, 2006, **128**, 14008.
- S. Demir, I.–R. Jeon, J.R. Long and T.D. Harris, *Coord. Chem. Rev.*, 2015, **289-290**, 149.
- J. D. Rinehart, M. Fang, W. J. Evans and J. R. Long, *Nat. Chem.*, 2011, **3**, 538; N. G. R. Hearn, K. E. Preuss, J. F. Richardson and S. Bin-Salamon, *J. Am. Chem. Soc.*, 2004, **126**, 9942; A. Caneschi, A. Dei, D. Gatteschi, L. Sorace and K. Vostrikova, *Angew. Chem. Int. Ed.*, 2000, **39**, 246; C. Benelli, A. Caneschi, D. Gatteschi, L. Pardi and P. Rey, *Inorg. Chem.*, 1989, **28**, 275.
- T. Kanetomo and T. Ishida, *Inorg. Chem.*, 2014, **53**, 10794.
- J.–P. Costes, F. Dahan, A. Dupuis and J.–P. Laurent, *Chem. Eur. J.*, 1998, **9**, 1616; M. L. Kahn, C. Mathonière and O. Kahn, *Inorg. Chem.*, 1999, **38**, 3692; M. Towatari, K. Nishi, T. Fujinami, N. Matsumoto, Y. Sunatsuki, M. Kojima, N. Mochida, T. Ishida, N. Re and J. Mrozinski, *Inorg. Chem.*, 2013, **52**, 6160; A. Okazawa, T. Shimada, N. Kojima, S. Yoshii, H. Nojiri and T. Ishida, *Inorg. Chem.*, 2013, **52**, 13351.
- R. D. Shannon and C. T. Prewitt, *Acta Crystallogr., Sect. B*, 1969, **25**, 925; R. D. Shannon, *Acta Crystallogr., Sect. A*, 1976, **32**, 751.
- M. Llunell, D. Casanova, J. Circa, J. M. Bofill, P. Alcmay, S. Alvarez, M. Pinsky and D. Avnir, *SHAPE*, v2.1, University of Barcelona and The Hebrew University of Jerusalem: Barcelona, 2005.
- J.–P. Sutter, M. L. Kahn and O. Kahn, *Adv. Mater.*, 1999, **11**, 863; M. L. Kahn, J. –P. Sutter, S. Golhen, P. Guionneau, L. Ouahab, O. Kahn and D. Chasseau, *J. Am. Chem. Soc.*, 2000, **122**, 3413.
- T. Mochizuki, T. Nogami and T. Ishida, *Inorg. Chem.*, 2009, **48**, 2254.
- W. Wong and S. F. Watkins, *J. Chem. Soc., Chem. Commun.*, 1973, 888.
- T. Ishida, R. Murakami, T. Kanetomo and H. Nojiri, *Polyhedron*, 2013, **66**, 183.
- R. Murakami, T. Ishida, S. Yoshii and H. Nojiri, *Dalton Trans.*, 2013, **42**, 1396.
- M. L. Baker, T. Tanaka, R. Murakami, S. Ohira-Kawamura, K. Nakajima, T. Ishida and H. Nojiri, *Inorg. Chem.*, 2015, in press. Doi: 10.1021/acs.inorgchem.5b00300.
- T. Ishida, R. Watanabe, K. Fujiwara, A. Okazawa, N. Kojima, G. Tanaka, S. Yoshii, H. Nojiri, *Dalton Trans.*, 2012, **41**, 13609; R. Watanabe, K. Fujiwara, A. Okazawa, G. Tanaka, S. Yoshii, H. Nojiri and T. Ishida, *Chem. Commun.*, 2011, **47**, 2110; T. Shimada, A. Okazawa, N. Kojima, S. Yoshii, H. Nojiri and T. Ishida, *Inorg. Chem.*, 2011, **50**, 10555; A. Okazawa, T. Shimada, N. Kojima, S. Yoshii, H. Nojiri, T. Ishida, *Inorg. Chem.*, 2013, **52**, 13351.
- H. Nojiri, K. –Y. Choi and N. Kitamura, *J. Magn. Magn. Mater.*, 2007, **310**, 1468.
- S. L. Castro, Z. Sun, C. M. Grant, J. C. Bollinger, D. N. Hendrickson and G. Christou, *J. Am. Chem. Soc.*, 1998, **120**, 2365; M. Sugita, N. Ishikawa, T. Ishikawa, S.–y. Koshihara and Y. Kaizu, *Inorg. Chem.*, 2006, **45**, 1299.
- K. S. Cole and H. R. Cole, *J. Chem. Phys.*, 1941, **9**, 341.
- R. Sessoli and A. K. Powell, *Coord. Chem. Rev.*, 2009, **253**, 2328.
- R. Sessoli, H.–L. Tsai, A. R. Schake, S. Wang, J. B. Vincent, K. Folting, D. Gatteschi, G. Christou and D. N. Hendrickson, *J. Am. Chem. Soc.* 1993, **115**, 1804.
- J. D. Rinehart and J. R. Long, *Chem. Sci.*, 2011, **2**, 2078.
- M. A. Aldamen, S. Cardona-Serra, J. M. Clemente-Juan, E. Coronado, A. Gaita-Arino, C. Martí-Gastaldo, F. Luis and O. Montero, *Inorg. Chem.*, 2009, **48**, 3467; J. J. Baldovi, S. Cardona-Serra, J. M. Clemente-Juan, E. Coronado, A. Gaita-Arino and A. Palií, *Inorg. Chem.*, 2012, **51**, 12565; G. F. Xu, Q.

- L. Wang, P. Gamez, Y. Ma, R. Clérac, J. Tang, S. P. Yan, P. Cheng and D. Z. Liao, *Chem. Commun.*, 2010, **46**, 1506; X. –L. Wang, L. –C. Li and D. –Z. Liao, *Inorg. Chem.*, 2010, **49**, 4735.
- V. Chandrasekhar, P. Bag, M. Speldrich, J. van Leusen and P. Kögerler, *Inorg. Chem.*, 2013, **52**, 5035.
- 26 N. Ishikawa, M. Sugita, N. Tanaka, T. Ishikawa, S.-y. Koshihara and Y. Kaizu, *Inorg. Chem.*, 2004, **43**, 5498.
- 27 N. Ishikawa, M. Sugita and W. Wernsdorfer, *Angew. Chem. Int. Ed.*, 2005, **44**, 2931.
- 28 T. Fukuda, K. Matsumura and N. Ishikawa, *J. Phys. Chem. A*, 2013, **117**, 10447.
- 29 E. M. Pineda, N. F. Chilton, F. Tuna, R. E. P. Winpenny and E. J. L. McInnes, *Inorg. Chem.*, 2015, in press. Doi: 10.1021/acs.inorgchem.5b00746.
- 30 M. Gonidec, E. S. Davies, J. McMaster, D. B. Amabilino and J. Veciana, *J. Am. Chem. Soc.*, 2010, **132**, 1756.
- 31 M. F. Richardson, W. F. Wagner and D. E. Sands, *J. Inorg. Nucl. Chem.*, 1968, **30**, 1275.
- 32 S. E. Denmark, Y. Fan and M. D. Eastgate, *J. Org. Chem.*, 2005, **70**, 5235.
- 33 *CrystalStructure* version 4.0, Rigaku Corp., Tokyo, Japan, 2010.